Dynamic apico-basal enrichment of the F-actin during cytokinesis in Arabidopsis cells embedded in their tissues

Author for correspondence:
M.-C. Caillaud,
E-mail: marie-cecile.caillaud@ens-lyon.fr

Alexis Lebecq, Aurélie Fangain, Alice Boussaroque and Marie-Cécile Caillaud[ID]

Laboratoire Reproduction et Développement des Plantes, Université de Lyon, ENS de Lyon, UCB Lyon 1, CNRS, INRA, Lyon, France

Abstract

Cell division is a tightly regulated mechanism, notably in tissues where malfunctions can lead to tumour formation or developmental defects. This is particularly true in land plants, where cells cannot relocate and therefore cytokinesis determines tissue topology. In plants, cell division is executed in radically different manners than in animals, with the appearance of new structures and the disappearance of ancestral mechanisms. Whilst F-actin and microtubules closely co-exist, recent studies mainly focused on the involvement of microtubules in this key process. Here, we used a root tracking system to image the spatio-temporal dynamics of both F-actin reporters and cell division markers in dividing cells embedded in their tissues. In addition to the F-actin accumulation at the phragmoplast, we observed and quantified a dynamic apico-basal enrichment of F-actin from the prophase/metaphase transition until the end of the cytokinesis.

1. Introduction

During plant mitosis, the cytoskeleton is reorganised in plant-specific structures that allow the separation of the mother cell into two daughter cells by the centrifugal growth of a new wall. Whilst the role of the actin cytoskeleton is of prime importance for animal cell division, the green cells require mostly microtubules in the early step of the cell division. Indeed, the plant cells can divide in the absence of F-actin (Baluska et al., 2001; Nishimura et al., 2003) and division still occurs in the presence of mutations in genes encoding actin or various actin-associated proteins (Jürgens, 2005). Before mitosis, the migration of the nucleus is not prevented by the cytochalasin D, a drug that disrupted the actin filaments (F-actin), suggesting that microtubules play an important role in this process (Katsuta et al., 1990). Yet, the actin cytoskeleton is found early during division with the formation of an actin ring at the cortex of the cell in preprophase, the actin preprophase band (PPB) which is considered to be wider than the microtubules PPB (Palevitz, 1987).

The formation of actin PPB depends on microtubules because the application of microtubules-depolymerizing drugs prevents the formation of both the microtubules and F-actin components of the PPB (Palevitz, 1987). However, actin PPB can also affect the microtubules PPB because actin depolymerisation results in drastic enlargement of the microtubules PPB and fluctuating division planes (Mineyuki & Palevitz, 1990). As the microtubules PPB narrows, the actin PPB narrows, and when the microtubules PPB reach their narrowest configuration, the fluorescence signals of F-actin start to disappear from the cell cortex region occupied by the microtubules PPB, giving rise to the actin-depleted zone (Cleary et al., 1992; Liu & Palevitz, 1992). In tobacco BY-2 cell culture cells, this actin-depleted zone is unambiguously visible and flanked by enrichments of F-actin whilst this depleted zone was not yet visualised in plant cells embedded in their tissues. Whether the actin-depleted zone coincides with the cortical division zone which acts as a landmark for the future cell division site is still unclear. Nevertheless, the actin-depleted zone is short-lived from metaphase through the anaphase/telophase transition (Clayton & Lloyd, 1985; Kakimoto & Shibaoka, 1987).

Whilst cytokinesis is progressing, the phragmoplast that guides the delivery of vesicles to form the expanding cell plate is composed of both microtubules and actin filaments (Staehelin & Hepler, 1996). Live-cell imaging over time in BY2 cells revealed that F-actin was involved in endoplasmic reticulum accumulation in the phragmoplast at the late phase (Higaki et al., 2008). Tobacco BY-2 cells treated with F-actin-depolymerizing drugs show disorganised phragmoplasts and wrinkled cell plates (Higaki et al., 2008; Hoshino et al., 2003; Kojo et al., 2013; Sano et al., 2005; Yoneda et al., 2004), which uncover the role of the F-actin during plant cytokinesis.

Because F-actin and microtubules closely co-exist and play important roles in the phragmoplast (Smith, 1999), cooperation or interaction between actin and microtubules cytoskeletons is assumed, and several proteins have been proposed to mediate the cooperation or interaction between actin and microtubules cytoskeletons (Buschmann et al., 2011; Igarashi et al., 2000; Klotz & Nick, 2012; Maeda et al., 2020; Schwab et al., 2003). In particular, the moss myosin VIII, a motor protein that interacts with both actin and microtubules, localises to the division site and the phragmoplast, linking microtubules to the cortical division zone via actin cytoskeleton (Wu & Bezanilla, 2014). These findings, together with other reports in which drug treatments and localization studies were performed (Lloyd & Traas, 1988; Molchan et al., 2002; Takeuchi et al., 2016), highlight that the actin cytoskeleton may interact with the microtubules bridging the cell cortex and the phragmoplast during cytokinesis.

Early work using immunolocalization and gold immuno-labelling of the actin cytoskeleton revealed the presence of a meshwork of F-actin that concentrated at the cortex of the cell, on the side facing the spindle poles (Cho & Wick, 1991; Mole-Bajer et al., 1988, Caillaud 2022). Recently, super-resolved imaging of the F-actin was performed using a photo-activatable Lifeact, a 17-amino-acid peptide that stained F-actin structures in BY2 cells (Durst et al., 2014). Using this approach, a gradient of the Lifeact–psRFP signal was observed that progressively led to a clear increase of signal intensity towards the cell poles, especially during the later mitotic phases (Durst et al., 2014). However, the dynamic of such polarisation was not yet reported in dividing plant cells surrounded by its tissue.

Here, we used our recently developed root tracking system to follow actin dynamics in dividing Arabidopsis meristematic root cells. By the visualisation of the fluorescent-tagged Lifeact together with cell division markers, we observed an apico-basal accumulation of the F-actin from the prophase/anaphase transition until the late stage of cytokinesis in Arabidopsis root meristematic cells. The role and the possible actors responsible for this actin enrichment are discussed.

2. Methods

2.1. Growth condition and plant materials

Arabidopsis Columbia-0 (Col-0) accession was used as a reference genomic background throughout this study. *Arabidopsis* seedlings *in vitro* on half Murashige and Skoog (½ MS) basal medium supplemented with 0.8% plant agar (pH 5.7) in continuous light conditions at 21°C. Plants were grown in soil under long-day conditions at 21°C and 70% humidity 16 hr daylight.

Table 1. Transgenic lines used in this study.

Construct	Ecotype	Reference	Resistance
Ub10pro:Lifeact-YFPv	Col-0	Doumane et al. (2021)	Basta
RPS5apro:Lifeact-TdTomato	Col-0	Liao and Weijers (2018)	Basta
Ub10pro:Lifeact-2xmTU2	Col-0	This study	Kana
KNOLLEpro:YFP-KNOLLE	Ler/Niederzenz-0 background	El Kasmi et al. (2013)	Basta
UB10pro:GFP-PHGAP1	Col-0	Stockle et al. (2016)	Basta
Ub10pro:RFP-MBD	Col-0	Lipka et al. (2014)	Basta
mGFP-ABD2	Col-0	N799991	Basta

2.2. Cloning

The lifeact sequence was flanked with attB2R and attB3 sequences and recombined by BP gateway reaction into pDONR221. Final destination vectors (UBQ10prom/P5', LifeAct/pDON221, 2xmTU2/pDONR-P3') were obtained using three fragments LR recombination system (life technologies, www.lifetechnologies.com/) using pK7m34GW destination vector (Karimi et al., 2007).

2.3. Plant materials

The transgenic lines used in this study are described in the Table 1.

2.4. Spinning-disk microscopy imaging

Images of the time-lapse images were acquired with the following spinning disk confocal microscope set up: inverted Zeiss microscope (AxioObserver Z1, Carl Zeiss Group, http://www.zeiss.com/) equipped with a spinning disk module (CSU-W1-T3, Yokogawa, www.yokogawa.com) and a ProEM+ 1024B camera (Princeton Instrument, http://www.princetoninstruments.com; Figure 2 only) or CameraPrime 95B (www.photometrics.com) using a 63× Plan-Apochromat objective (numerical aperture 1.4, oil immersion). The mTURQUOISE2 was excited with a 445 nm laser (80 mW) and fluorescence emission was filtered by a 482/35 nm BrightLine single-band bandpass filter (Semrock, http://www.semrock.com/), GFP and mCITRINE were excited with a 488 nm laser (150 mW) and fluorescence emission was filtered by a 525/50 nm BrightLine! a single-band bandpass filter (Semrock), tdTom/RFP was excited with a 561 nm laser (80 mW) and fluorescence emission was filtered by a 609/54 nm BrightLine! a single-band bandpass filter (Semrock, http://www.semrock.com/). For quantitative imaging, pictures of epidermal root meristem cells were taken with detector settings optimised for low background and no pixel saturation. Care was taken to use similar confocal settings when comparing fluorescence intensity or for quantification. Root tracking experiments were performed as described in Doumane et al. (2017).

The fluorescence intensity was obtained using the Fiji tool. A line of 96 pixels was drawn through the cell and the intensity of grey was plotted using the Plot Profile tool. The values were transferred in Excel to obtain the graph.

2.5. Statistical analysis

For localization index analysis, one dividing cell and a non-dividing cell were taken for each root (17 roots). For every two cells, the signal intensity was measured for the Apico-basal membranes, the two laterals membranes, and in two elliptical regions of interest

Table 2. Statistical analysis corresponding to Figure 3c.

Kruskal–Wallis				
Model	Pair	χ^2	*df*	*p*-value
Actin localization index per membrane	Dividing cell	20.828	1	5.024e-06
	Non-dividing cells			

(ROIs) of the cytosol (Tables 2 and 3). Ratios were obtained by taking the average of the two measured intensities. Localization index comparisons were performed using a Kruskal–Wallis rank sum test analysis in R (v. 3.6.1; R Core Team, 2019), using R studio interface and the packages ggplot2 (Wickham, 2016). Graphs were obtained with R and R-studio software and customised with Inkscape (https://inkscape.org).

For F-actin accumulation analysis (Figure 3e), 2 hr time-lapse (2 min intervals between each acquisition) were made on 7 roots and 25 cells, at different dividing steps, were taken for the analysis. For each division figure, the image in which the dividing cell is at its maximum volume was extracted to perform a localization index (as previously described except that no non-dividing cells were taken). We consider PPB cells that do not enter in the division during the time-laps as 'young PPBs' and those who did as 'old PPBs'. The 'old PPBs' localization index was performed between 6 and 2 min before nuclear envelope break. Statistical analyses were performed exactly as for Figure 3c,d (Table 4).

3. Results

In order to analyse in vivo the behaviours of the actin cytoskeleton in a dividing tissue, we collected a set of Lifeact fluorescent reporters (Table 1), tagged with YFPv (Doumane et al., 2021), tdTomato (Liao & Weijers, 2018). We generated a blue-tagged version of Lifeact with 2xmTURQUOISE2 (2xmTU2) under a Ub10 promoter (*Ub10pro:Lifeact-2xmTU2*). Using the recently developed root tracking system, we observed the behaviour of the actin cytoskeleton every 3 min in epidermal cells of Arabidopsis up to five root tips in one experiment, in three dimensions, using a spinning disk confocal microscope (Doumane et al., 2017). We first analysed in time-lapse Arabidopsis meristematic root cells during division in plants expressing the actin marker *Lifeact-YFPv* (Figure 1). The *z*-projection of division tissues expressing the actin marker Lifeact-YFPv showed that during cytokinesis, the F-actin is clearly observed in the developing phragmoplast (Figure 1, empty arrows). Moreover, an apico-basal accumulation of Lifeact-YFPv during cytokinesis was visible in the dividing root tissues (Figure 1, white plain arrows), as it was previously reported (Voigt et al., 2005).

We confirmed the F-actin patterning during cell division obtained with the LifeAct-YFPv reporter with another well-characterised F-actin biosensor. We performed the same analysis with plants expressing the C-terminal half of the plant Fimbrin-like gene AtFim1 (aa 325–687) fused to the mGFP fluorescent protein (m*GFP-ABD2*). Time-lapse analysis of the growing root Arabidopsis meristem expressing m*GFP-ABD2* displayed the same apico-basal accumulation of F-actin during cytokinesis (Figure 2).

We confirmed this result by projecting in the *z*-plane the cells and by changing the orientation to enable the observation of the apical–basal face of the dividing cell (Figure 3a). Using this approach, we confirmed that whilst the phragmoplast was extending, the Lifeact-2xmTU2 signal covered the entire apico-basal plane of the cell whilst no accumulation was observed in the lateral part of the cell (Figure 3b). During phragmoplast expansion, the signal at the apico-basal part of the cell stayed strong before the decrease in the fluorescence signal could be observed at the end of the cytokinesis (Figures 1–3).

We quantified the observed signal in the Arabidopsis line expressing *LifeAct-2xmTU2* in dividing cell and non-dividing cells. To do so, we analysed using ImageJ the ratio of fluorescence intensity between the two apical and basal parts of the cell and the fluorescence intensity in the lateral parts of the cell (Figure 3b,c). We surveyed the ratio of fluorescence intensity between the apico-basal part of the cell and the cytoplasm from dividing cell and non-dividing cells (Figure 3b–d). Using this quantitative approach, we confirmed the enrichment of the F-actin signal at the apico-basal part of the dividing cells, whilst no specific distribution was observed in non-dividing cells (Figure 3b–d and Tables 2 and 3).

Table 3. Statistical analysis corresponding to Figure 3d.

Kruskal–Wallis				Post Dunn test, method 'Bonferroni'	
Model	χ^2	*df*	*p*-value	Pair	*p*-value
Actin localization index per cytosol	32.576	3	3.957e-06	Apico-basal parts of dividing cells/cytosol	.0000*
				Lateral parts of dividing cells/cytosol	
				Apico-basal parts of dividing cells/cytosol	.0174*
				Apico-basal parts of non-dividing cells/cytosol	
				Apico-basal parts of dividing cells/cytosol	.0004*
				Lateral parts of non-dividing cells/cytosol	
				Lateral parts of dividing cells/cytosol	.0149*
				Apico-basal parts of non-dividing cells/cytosol	
				Lateral parts of dividing cells/cytosol	.2305
				Lateral parts of non-dividing cells/cytosol	
				Apico-basal parts of non-dividing cells/cytosol	.8940
				Lateral parts of non-dividing cells/cytosol	

Note: Comparison of all the conditions together using Kruskal–Wallis is reported in the left part of the table, whilst pair comparison after Kruskal–Wallis analysis using post Dunn test, method 'Bonferroni', are presented in the right part of the table.
*The start highlights results with statistical differences.

Table 4. Statistical analysis corresponding to Figure 3e.

Kruskal–Wallis				Dunn test, method 'Bonferroni'	
Model	χ^2	df	p-value	Pair	p-value
Dissociation index (membranes apical–basal/laterals)	26.0773	6	0	Young PPB Old PPB	.1406
				Young PPB Nuclear envelop break	.0095*
				Young PPB Spindle formation	.0001*
				Young PPB Metaphase–anaphase transition	.0002*
				Young PPB Solid phragmoplast	.0016*
				Young PPB Ring phragmoplast	.0009*
				Old PPB Nuclear envelop break	1
				Old PPB Spindle formation	.3283
				Old PPB Metaphase–anaphase transition	.5766
				Old PPB Solid phragmoplast	1
				Old PPB Ring phragmoplast	1
				For every other combination	1

Note: Comparison of all the conditions together using Kruskal–Wallis is reported in the left part of the table, whilst pair comparison after Kruskal–Wallis analysis using post Dunn test, method 'Bonferroni', are presented in the right part of the table.
*The start highlights results with statistical differences.

To address whether the 'actin-depleted zone' was quantifiable, we analysed the ratio of fluorescence intensity between the lateral part of the cell and the cytoplasm for dividing cell and non-dividing cells (Figure 3b–d). Whilst a slight decrease in the ratio was observed for the dividing cells compared to non-dividing cells, the presence of the adjacent non-dividing cells surrounding this region might mask a clear depletion. Indeed, whilst the actin-depleted zone is clearly observed in cell culture (Cleary et al., 1992; Liu & Palevitz, 1992), this depleted zone is difficult to image in dividing tissue (Voigt et al., 2005).

To uncover when the accumulation of the F-actin at the apico-basal part of the cell occurs, we analysed the signal collected from plant co-expressing *Lifeact-YFPv* and *RFP-MBD* at key steps of the cell division. Images extracted from time-lapse analysis or from single acquisitions were quantified for the Lifeact-YFPv signal at the apico-basal part of the cell and compared with the signal observed in the lateral parts of the cell, using the signal corresponding to the microtubules as reference for mitotic figures (Figure 3e, Table 4 and Supplemental Movie S1). We showed a gradual enrichment of the fluorescent signal corresponding to F-actin at the apico-basal part of the dividing cell during the spindle formation, where the difference in intensity was at its climax (Figure 3e and Table 4). Based on these quantifications, we conclude that the apico-basal accumulation of F-actin appears during prophase/metaphase transition and persists until the end of the cytokinesis in Arabidopsis root meristem.

Using plant co-expressing *Lifeact-tdTom* and the cell plate marker *YFP-KNOLLE*, we tracked dividing cells in the root meristem from early metaphase. An increase of the signal could be observed on the lateral parts of the cell, flanking the cortical division zone, but the signal in the surrounding cell was masking the signal from the dividing cells (Figure 4, white arrows). Therefore, it did not allow us to certify that this signal corresponds to the earlier described 'actin twin peaks' (Smertenko et al., 2010). As soon as YFP-KNOLLE was found enriched in the developing cell plate, the lateral signal corresponding to Lifeact-tdTom disappeared and the rapid accumulation of Lifeact-tdTom signal at the apico-basal part of the cell was observed, as well as in the phragmoplast (Figure 4a,b). This accumulation of F-actin at the apico-basal part of the dividing cell was stable during cell plate expansion as YFP-KNOLLE signal expanded towards the cell periphery (Figure 4a,b). When the cell plate was fully attached to the mother cell leading to the formation of the crosswall, no more accumulation of the F-actin at the apico-basal parts of the cell could be observed using the Lifeact-tdTom reporter line (Figure 4a,b). At this stage, the cable of F-actin was found in the cytoplasm of newly formed daughter cells (Figure 4).
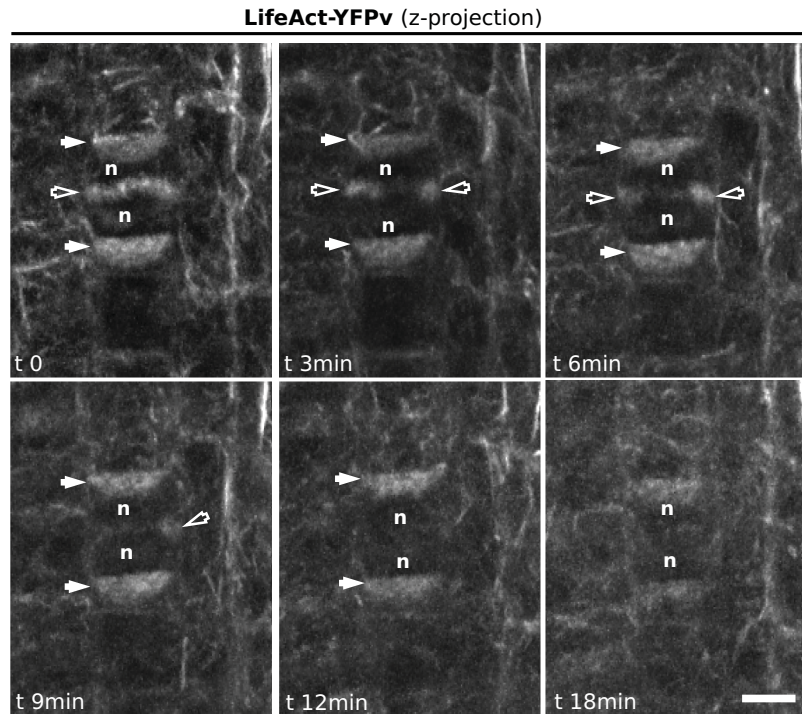
LifeAct-YFPv (z-projection)

Fig. 1. Representatives images of a z-projection of a time-lapse analysis in Arabidopsis root meristem, expressing *Ub10:Lifeact-YFPv*. White arrows, F-actin enrichment at the apico-basal part of the cells; empty arrows, F-actin in the phragmoplast; n, nucleus. Scale bar = 5 μm.
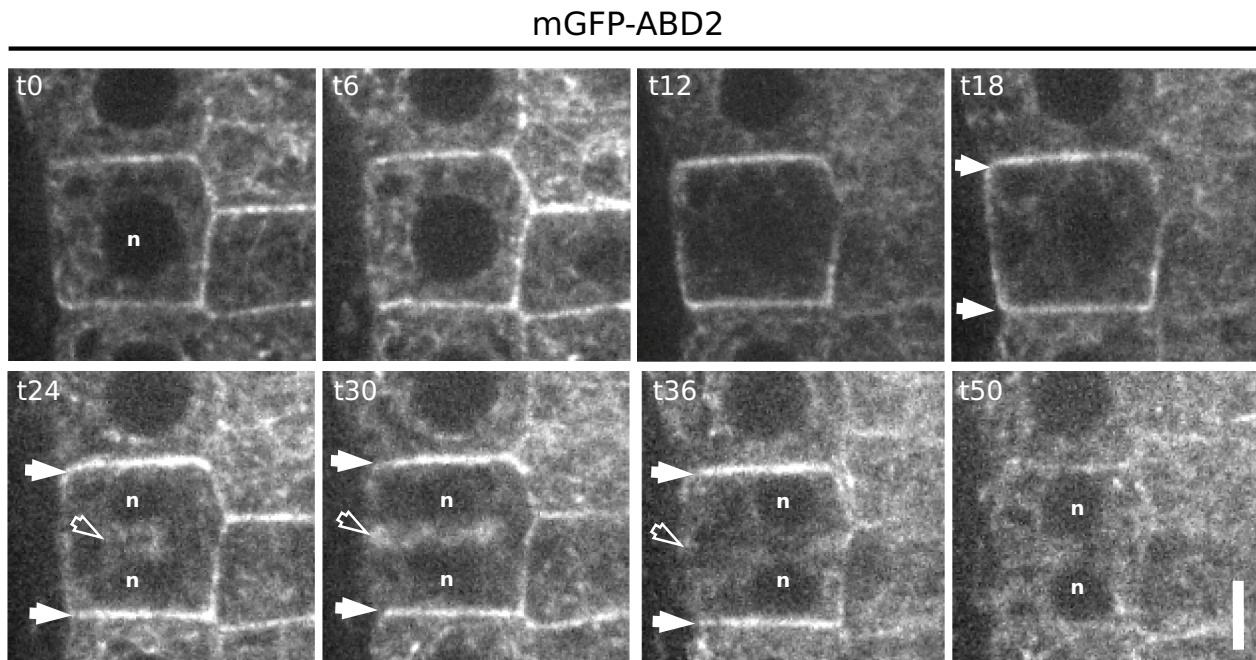
mGFP-ABD2

Fig. 2. Representatives images of a z-projection of a time-lapse analysis in Arabidopsis root meristem, expressing *mGFP-ABD2*. White arrows, F-actin enrichment at the apico-basal part of the cells; empty arrows, F-actin in the phragmoplast; n, nucleus. Scale bar = 5 μm.

We confirmed these results using an Arabidopsis line co-expressing a cortical division zone marker together with the F-actin reporter (Figure 5 and supplemental movie 2). In transgenic lines expressing *GFP–PHGAP1* under a *Ub10 promoter*, the fluorescent signal was reported to accumulate at the cortical division zone in metaphase/anaphase and remains throughout cytokinesis (Stockle et al., 2016). Dual localization of GFP-PHGAP1 and Lifeact-tdTom

showed that the accumulation at the apico-basal part of the dividing cells appeared before the signal corresponding to GFP-PHGAP1 could be noticed, suggesting that the F-actin polarisation appears before the recruitment of PHGAP1 at the CDZ (Figure 5).

Colocalization of F-actin using Lifeact-tdTom with mitotic microtubules decorated by RFP-MBD allowed used to visualise in detail the dynamics at the phragmoplast. During early anaphase,
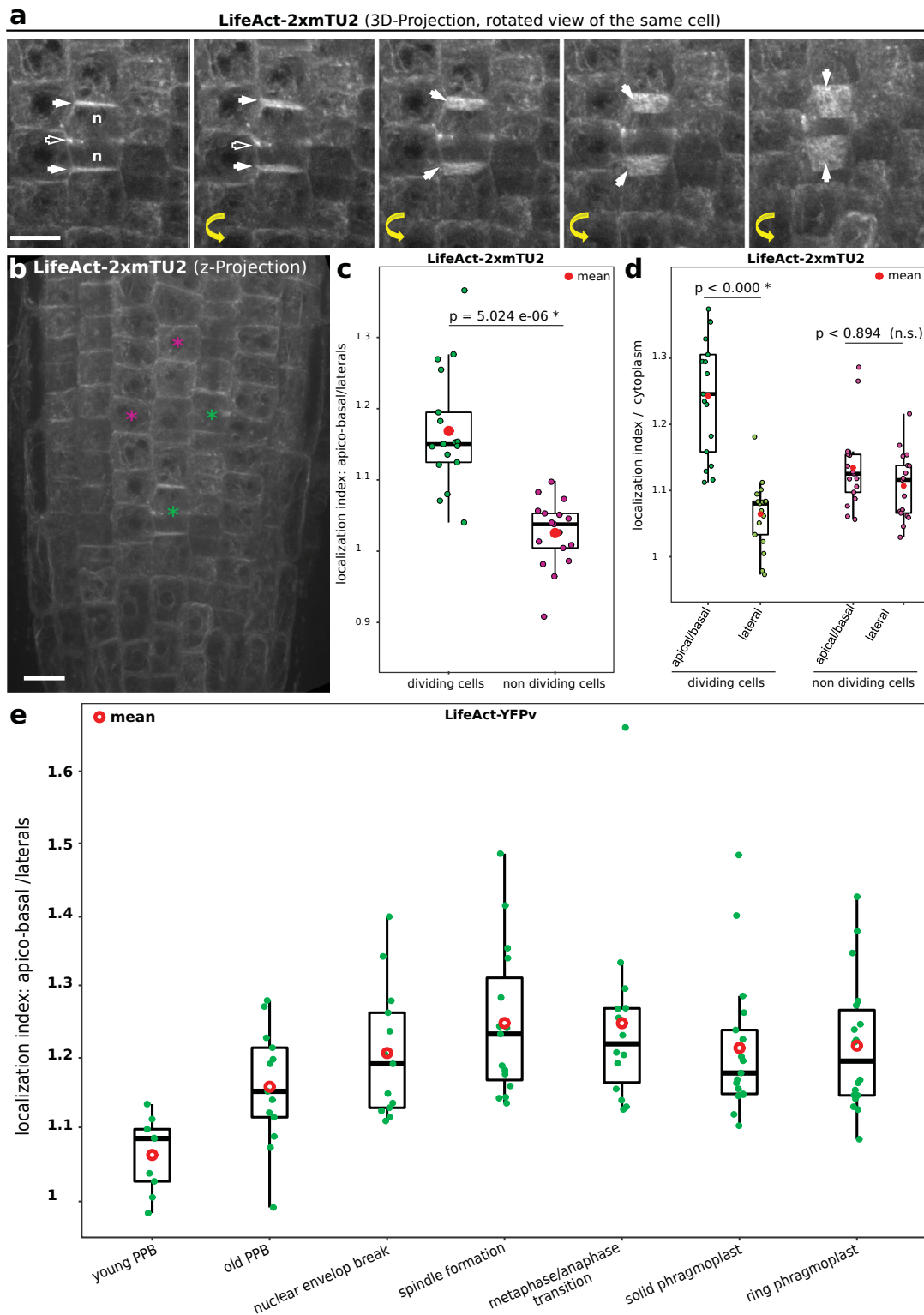
Fig. 3. (a) Representative images of a three-dimensional projection of a dividing cell in Arabidopsis root meristem expressing *Ub10:LifeAct-2xmTU2*. White arrows, F-actin enrichment at the apico-basal part of the cells; empty arrows, F-actin in the phragmoplast; n, nucleus. The yellow arrows marked the four rotated images obtained by the rotation in ImageJ of the initial *z*-projected image presented in the left panel. Scale bar = 10 μm. (b) Representative images of the distribution of LifeAct-2xmTU2 in dividing cell and non-dividing cells used for the quantification. Scale bar = 15 μm. (c) Quantification of the localization index of LifeAct-2xmTU2 between the apico-basal part of the cell and the lateral part of the cell of dividing versus non-dividing cells. (d) Quantification of the localization index of LifeAct-2xmTU2 between the apico-basal or the lateral part of the cell and the cytoplasm of dividing versus non-dividing cells. (e) Quantification of the localization index of LifeAct-YFPv between the apico-basal or the lateral part of the cells at key steps of the cell division, visualised thanks to the microtubule marker RFP-MBD. In the plots, the middle horizontal bars represent the median, whilst the bottom and top of each box represent the 25th and 75th percentiles, respectively. At most, the whiskers extend to 1.5 times the IQR and exclude data beyond that range. For the range of values under 1.5 times the IQR, the whiskers represent the range of maximum and minimum values.
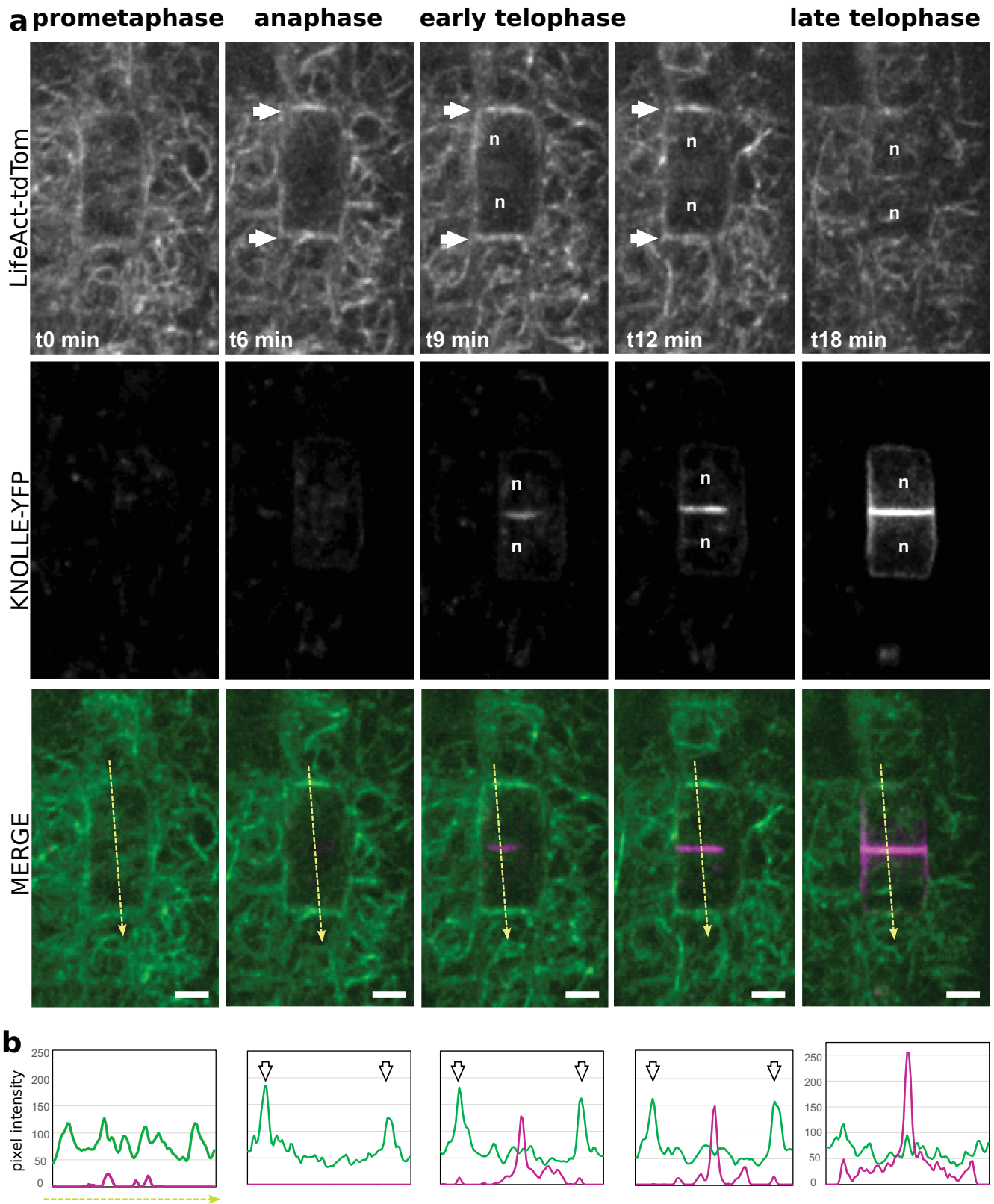
Fig. 4. (a) Representatives images of a time-lapse analysis in Arabidopsis root meristem, expressing *LifeAct-tdTom* (green) together with *KNOLLE-YFP* (magenta). (b) Semi-quantitative measurement of the signal intensity for both LifeAct-tdTom (green) and KNOLLE-YFP (magenta) along the yellow line. White arrows, F-actin enrichment at the apico-basal part of the cells; orange arrows, accumulation of F-actin in the phragmoplast; n, nucleus. Scale bar = 5 μm.
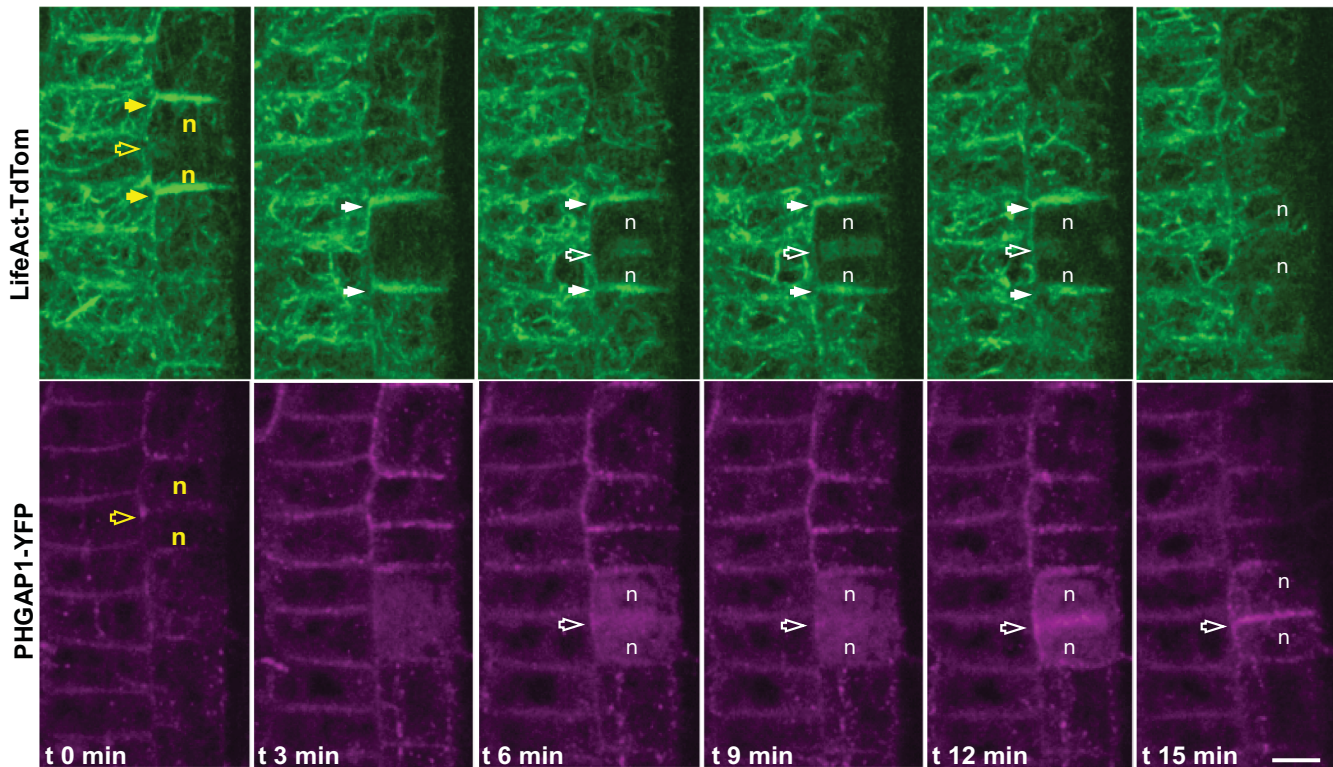
Fig. 5. Representatives images of a time-lapse analysis in Arabidopsis root meristem, expressing *LifeAct-tdTom* (green) together with *GFP-PHGAP1* (magenta). Yellow and white arrows, F-actin enrichment at the apico-basal part of the cells; empty arrows, the position of the cortical division zone; n, nucleus. Scale bar = 5 μm.

the colocalization of microtubules and F-actin was total whilst in late cytokinesis, colocalization analysis highlighted the differences in positioning of both cytoskeletons (Figure 6 and Supplemental Movie S1, S2). At the ring phragmoplast stage, the lifeact-tdTom preceded the RFP-MBD at the edge of the phragmoplast (Figure 6a,b and Supplemental Movie S1), confirming the role of F-actin in the phragmoplast guidance in the attachment phases of the cytokinesis.

4. Discussion

An extraordinary new view of the dynamic spatiotemporal regulation of key components of the cell division orientation is emerging from advances in live-cell imaging in Arabidopsis root meristem (Drevensek et al., 2012; Lipka et al., 2014; Muller et al., 2006; Schaefer et al., 2017; Stockle et al., 2016; Walker et al., 2007; Xu et al., 2008). However, when it comes to studying subcellular dynamics during plant cell division manual adjustment is required since the area under study will rapidly grow out of the field of view. This makes it necessary to obtain an automated system to release the biology researcher from spending up to a day in front of the microscope performing adjustments every 10 min. In the present study, we took advantage of a confocal chasing system to track the meristematic zone of the root based on point-to-point correspondences and motion estimation (Doumane et al., 2017). Using this approach, we can track over a long period (10 hr) mitosis in the meristem of multiple Arabidopsis roots by spinning disk confocal microscopy. This method allowed us to rapidly collect biological replicates on the behaviour of the actin cytoskeleton during plant cell division and to quantify it. We showed that, in addition to its localization in the phragmoplast, F-actin polarised

at the apico-basal parts of the cell from the prophase/metaphase transition and decreased at the end of the cytokinesis to eventually form actin cables in the cytoplasm of the two newly formed daughter cells. How this polar F-actin transient accumulation is achieved remains unclear.

In animal cytokinesis, the local increase in the level of the anionic lipid phosphatidylinositol-4,5-bisphosphate (PtdIns(4,5)P$_2$) modifies F-actin amounts at the cell equator and controls cytokinesis abscission (Dambournet et al., 2011). Using our root tracking system, we observed that PtdIns(4,5)P$_2$ has specific subcellular localization during plant cell division (Simon et al., 2016) suggesting a link between the proper spatial production of phosphoinositides and successful completion of cytokinesis. Moreover, the depletion of the PtdIns(4,5)P$_2$ from the plasma membrane using the iDePP system highlighted the importance of the PtdIns(4,5)P$_2$ pool for proper F-actin dynamics (Doumane et al., 2021). Actin nucleators such as ARP2/3 were shown to interact strongly with the plasma membrane in Arabidopsis (Kotchoni et al., 2009), and both ACTIN DEPOLYMERIZATION FACTOR (ADF)/cofilin and profilin bind to PtdIns(4,5)P$_2$ (Gungabissoon et al., 1998). In *Zea mays*, PROFILIN1 (ZmPRO1) inhibits hydrolysis of PtdIns(4,5)P$_2$ at the membrane by the membrane-associated enzyme Phospholipase C (Staiger et al., 1993). It was reported that PROFILIN from *Phaseolus vulgaris* could bind directly to the phosphoinositide enzyme PtdIns-3Kinase, which suggests that PROFILIN might participate in membrane trafficking, and acts as a linker between the endocytic pathway and the F-actin dynamics (Aparicio-Fabre et al., 2006).

In Arabidopsis, enzymes that locally produce PtdIns(4,5)P$_2$ named PIP5K1 and PIP5K2 were reported to be most active among the ubiquitously expressed PtdIns4P 5-kinases (Ischebeck
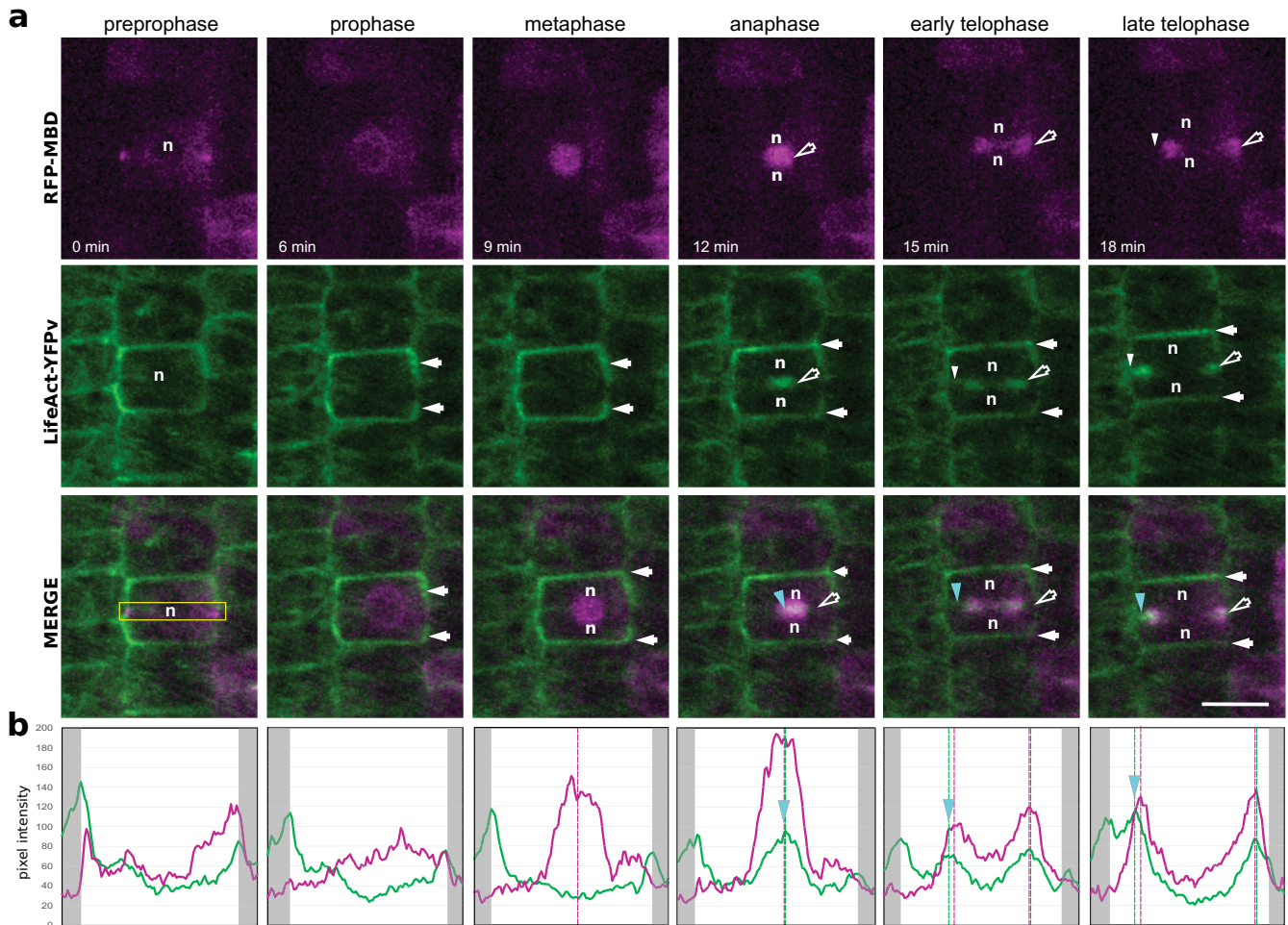
Fig. 6. (a) Representatives images of a time-lapse analysis in Arabidopsis root meristem, expressing *LifeAct-YFPv* (green) together with *RFP-MBD* (magenta). White arrows, F-actin enrichment; empty arrows, the phragmoplast; blue arrowhead, the position of the F-actin in the phragmoplast; n, nucleus. Scale bar = 10 μm. (b) Semi-quantitative analysis of the fluorescence intensity corresponding to LifeAct-YFPv (green) and RFP-MBD (magenta) in a rectangular ROI (h22xw106 pixels) represented in yellow on the merged image in (a). The grey area corresponds to the external part of the dividing cell and the blue arrowhead corresponds to the position of the F-actin in the phragmoplast.

et al., 2008) and therefore are likely making a major contribution to cellular PtdIns(4,5)P$_2$ formation (Tejos et al., 2014). During embryogenesis, double mutations in *pip5k1/pip5k2* bent to defects characterised by the formation of a vague apical-to-basal boundary (Tejos et al., 2014) which eventually lead to sterile plants (Tejos et al., 2014). Both YFP-PIP5K1 and YFP-PIP5K2 seem to be enriched in the apico-basal membrane in dividing cells (Ischebeck et al., 2013) as observed for the F-actin in the present study. Based on this observation, it is appealing to emphasise that the composition in phosphoinositides could mediate the F-actin polymerisation at the apico-basal part of the cell, allowing the polarisation of the cell during its division. However, their dynamic localization during cell division needs yet to be addressed in detail, to disentangle if those kinases locally increase PtdIns(4,5)P$_2$ production. It is even more intriguing since, in a previous report, we did not observe obvious polarity for the PtdIns(4,5)P$_2$ biosensor 2xPH^{PLC}-mCitrine using localization index analysis (Simon et al., 2016). However, because in this previous study (a) we did not distinguish between dividing cell and non-dividing cell, (b) the quantification was made on the transition zone between the meristem and the elongation zone of the root and (c) the actin-F polarisation in the dividing cell is observed in the meristematic part of the root, we cannot conclude about a possible relationship

between F-actin and PtdIns(4,5)P$_2$, and further investigation should be performed to address this point.

Why do cells in their tissues need this F-actin accumulation at their apico-basal parts? It is striking to observe, when it comes to cell division orientation, that in mutants impaired in the cortical dividing zone (CDZ) definition and/or microtubules PPB organisation, the defects rely on titled cell plates, yet the attachment is still happening in the lateral membranes of the root meristematic cells (Kumari et al., 2021; Muller et al., 2006; Schaefer et al., 2017; Stockle et al., 2016). In another word, in microtubule defective mutants impaired in PPB or CDZ formation, we do not observe the attachment of the cell plate in the apico-basal membranes. Challenging the F-actin accumulation at the apico-basal part of the cell might be the key to understanding how the cell polarity is maintained after microtubules cytoskeleton perturbation during cell division in plant tissues.

Acknowledgements

References

Aparicio-Fabre, R., Guillen, G., Estrada, G., Olivares-Grajales, J., Gurrola, G., & Sanchez, F. (2006). Profilin tyrosine phosphorylation in poly-L-proline-binding regions inhibits binding to phosphoinositide 3-kinase in Phaseolus vulgaris. *The Plant Journal: For Cell and Molecular Biology*, **47**, 491–500. https://doi.org/10.1111/j.1365-313X.2006.02787.x

Baluska, F., Jasik, J., Edelmann, H. G., Salajova, T., & Volkmann, D. (2001). Latrunculin B-induced plant dwarfism: Plant cell elongation is F-actin-dependent. *Developmental Biology*, **231**, 113–124. https://doi.org/10.1006/dbio.2000.0115

Buschmann, H., Green, P., Sambade, A., Doonan, J., & Lloyd, C. (2011). Cytoskeletal dynamics in interphase, mitosis and cytokinesis analysed through agrobacterium-mediated transient transformation of tobacco BY-2 cells. *New Phytologist*, **190**, 258–267.

Caillaud, M. C. (2022). Methods to Visualize the Actin Cytoskeleton During Plant Cell Division. In Plant Cell Division (pp. 1–16). Humana, New York, NY.

Cho, S. O., & Wick, S. M. (1991). Actin in the developing stomatal complex of winter rye: A comparison of actin antibodies and Rh-phalloidin labeling of control and CB-treated tissues. *Cell Motility and the Cytoskeleton*, **19**, 25–36.

Clayton, L., & Lloyd, C. W. (1985). Actin organization during the cell cycle in meristematic plant cells. Actin is present in the cytokinetic phragmoplast. *Experimental Cell Research*, **156**, 231–238. https://doi.org/10.1016/0014-4827(85)90277-0

Cleary, A., Gunning, B. E., Wasteneys, G. O., & Hepler, P. K. (1992). Microtubule and F-actin dynamics at the division site in living Tradescantia stamen hair cells. *Journal of Cell Science*, **103**, 977–988.

Dambournet, D., Machicoane, M., Chesneau, L., Sachse, M., Rocancourt, M., El Marjou, A., Formstecher, E., Salomon, R., Goud, B., & Echard, A. (2011). Rab35 GTPase and OCRL phosphatase remodel lipids and F-actin for successful cytokinesis. *Nature Cell Biology*, **13**, 981–988. https://doi.org/10.1038/ncb2279

Doumane, M., Lebecq, A., Colin, L., Fangain, A., Stevens, F. D., Bareille, J., Hamant, O., Belkhadir, Y., Munnik, T., Jaillais, Y., & Caillaud, M. C. (2021). Inducible depletion of PI(4,5)P2 by the synthetic iDePP system in Arabidopsis. *Nature Plants*, **7**, 587–597. https://doi.org/10.1038/s41477-021-00907-z

Doumane, M., Lionnet, C., Bayle, V., Jaillais, Y., & Caillaud, M. C. (2017). Automated tracking of root for confocal time-lapse imaging of cellular processes. *Bio-Protocol*, **7**, e2245. https://doi.org/10.21769/BioProtoc.2245

Drevensek, S., Goussot, M., Duroc, Y., Christodoulidou, A., Steyaert, S., Schaefer, E., Duvernois, E., Grandjean, O., Vantard, M., Bouchez, D., & Pastuglia, M. (2012). The Arabidopsis TRM1-TON1 interaction reveals a recruitment network common to plant cortical microtubule arrays and eukaryotic centrosomes. *Plant Cell*, **24**, 178–191. https://doi.org/10.1105/tpc.111.089748

Durst, S., Hedde, P. N., Brochhausen, L., Nick, P., Nienhaus, G. U., & Maisch, J. (2014). Organization of perinuclear actin in live tobacco cells observed by PALM with optical sectioning. *Journal of Plant Physiology*, **171**, 97–108. https://doi.org/10.1016/j.jplph.2013.10.007

El Kasmi, F., Krause, C., Hiller, U., Stierhof, Y. D., Mayer, U., Conner, L., . . . & Jürgens, G. (2013). SNARE complexes of different composition jointly mediate membrane fusion in Arabidopsis cytokinesis. *Molecular biology of the cell*, **24**(10), 1593–1601.

Gungabissoon, R. A., Jiang, C.-J., Drbak, B. K., Maciver, S. K., & Hussey, P. J. (1998). Interaction of maize actin-depolymerising factor with actin and phosphoinositides and its inhibition of plant phospholipase C. *The Plant Journal*, **16**, 689–696. https://doi.org/10.1046/j.1365-313x.1998.00339.x

Higaki, T., Kutsuna, N., Sano, T., & Hasezawa, S. (2008). Quantitative analysis of changes in actin microfilament contribution to cell plate development in plant cytokinesis. *BMC Plant Biology*, **8**, 80. https://doi.org/10.1186/1471-2229-8-80

Hoshino, H., Yoneda, A., Kumagai, F., & Hasezawa, S. (2003). Roles of actin-depleted zone and preprophase band in determining the division site of higher-plant cells, a tobacco BY-2 cell line expressing GFP-tubulin. *Protoplasma*, **222**, 157–165. https://doi.org/10.1007/s00709-003-0012-8

Igarashi, H., Orii, H., Mori, H., Shimmen, T., & Sonobe, S. (2000). Isolation of a novel 190 kDa protein from tobacco BY-2 cells: Possible involvement in the interaction between actin filaments and microtubules. *Plant and Cell Physiology*, **41**, 920–931.

Ischebeck, T., Stenzel, I., & Heilmann, I. (2008). Type B phosphatidylinositol-4-phosphate 5-kinases mediate Arabidopsis and *Nicotiana tabacum* pollen tube growth by regulating apical pectin secretion. *The Plant Cell*, **20**, 3312–3330. https://doi.org/10.1105/tpc.108.059568

Ischebeck, T., Werner, S., Krishnamoorthy, P., Lerche, J., Meijon, M., Stenzel, I., Lofke, C., Wiessner, T., Im, Y. J., Perera, I. Y., Iven, T., Feussner, I., Busch, W., Boss, W. F., Teichmann, T., Hause, B., Persson, S., & Heilmann, I. (2013). Phosphatidylinositol 4, 5-bisphosphate influences PIN polarization by controlling clathrin-mediated membrane trafficking in Arabidopsis. *The Plant Cell*, **25**, 4894–4911. https://doi.org/10.1105/tpc.113.116582

Jürgens, G. (2005). Cytokinesis in higher plants. *Annual Review of Plant Biology*, **56**, 281–299.

Kakimoto, T., & Shibaoka, H. (1987). Actin filaments and microtubules in the preprophase band and phragmoplast of tobacco cells. *Protoplasma*, **140**, 151–156.

Karimi, M., Depicker, A., & Hilson, P. (2007). Recombinational cloning with plant gateway vectors. *Plant Physiology*, **145**, 1144–1154. https://doi.org/10.1104/pp.107.106989

Katsuta, J., Hashiguchi, Y., & Shibaoka, H. (1990). The role of the cytoskeleton in positioning of the nucleus in premitotic tobacco BY-2 cells. *Journal of Cell Science*, **95**, 413–422.

Klotz, J., & Nick, P. (2012). A novel actin-microtubule cross-linking kinesin, NtKCH, functions in cell expansion and division. *The New Phytologist*, **193**, 576–589. https://doi.org/10.1111/j.1469-8137.2011.03944.x

Kojo, K. H., Higaki, T., Kutsuna, N., Yoshida, Y., Yasuhara, H., & Hasezawa, S. (2013). Roles of cortical actin microfilament patterning in division plane orientation in plants. *Plant & Cell Physiology*, **54**, 1491–1503. https://doi.org/10.1093/pcp/pct093

Kotchoni, S. O., Zakharova, T., Mallery, E. L., Le, J., El-Assal Sel, D., & Szymanski, D. B. (2009). The association of the Arabidopsis actin-related protein2/3 complex with cell membranes is linked to its assembly status but not its activation. *Plant Physiology*, **151**, 2095–2109. https://doi.org/10.1104/pp.109.143859

Kumari, P., Dahiya, P., Livanos, P., Zergiebel, L., Kölling, M., Poeschl, Y., Stamm, G., Hermann, A., Abel, S., & Müller, S. (2021). IQ67 DOMAIN

proteins facilitate preprophase band formation and division-plane orientation. *Nature Plants*, **7**, 739–747.

Liao, C. Y., & **Weijers, D.** (2018). A toolkit for studying cellular reorganization during early embryogenesis in *Arabidopsis thaliana*. *The Plant Journal*, **93**, 963–976.

Lipka, E., **Gadeyne, A.**, **Stockle, D.**, **Zimmermann, S.**, **De Jaeger, G.**, **Ehrhardt, D. W.**, **Kirik, V.**, **Van Damme, D.**, & **Muller, S.** (2014). The Phragmoplast-orienting Kinesin-12 class proteins translate the positional information of the preprophase band to establish the cortical division zone in *Arabidopsis thaliana*. *Plant Cell*, **26**, 2617–2632. https://doi.org/10.1105/tpc.114.124933

Liu, B., & **Palevitz, B. A.** (1992). Organization of cortical microfilaments in dividing root cells. *Cell Motility and the Cytoskeleton*, **23**, 252–264.

Lloyd, C. W., & **Traas, J.** (1988). The role of F-actin in determining the division plane of carrot suspension cells. *Drug Studies. Development*, **102**, 211–221.

Maeda, K., **Sasabe, M.**, **Hanamata, S.**, **Machida, Y.**, **Hasezawa, S.**, & **Higaki, T.** (2020). Actin filament disruption alters phragmoplast microtubule dynamics during the initial phase of plant cytokinesis. *Plant and Cell Physiology*, **61**, 445–456.

Mineyuki, Y., & **Palevitz, B.** (1990). Relationship between preprophase band organization, F-actin and the division site in allium: Fluorescence and morphometric studies on cytochalasin-treated cells. *Journal of Cell Science*, **97**, 283–295.

Molchan, T. M., **Valster, A. H.**, & **Hepler, P. K.** (2002). Actomyosin promotes cell plate alignment and late lateral expansion in Tradescantia stamen hair cells. *Planta*, **214**, 683–693.

Mole-Bajer, J., **Bajer, A. S.**, & **Inoue, S.** (1988). Three-dimensional localization and redistribution of F-actin in higher plant mitosis and cell plate formation. *Cell Motility and the Cytoskeleton*, **10**, 217–228. https://doi.org/10.1002/cm.970100126

Muller, S., **Han, S.**, & **Smith, L. G.** (2006). Two kinesins are involved in the spatial control of cytokinesis in Arabidopsis thaliana. *Current Biology*, **16**, 888–894. https://doi.org/10.1016/j.cub.2006.03.034

Nishimura, T., **Yokota, E.**, **Wada, T.**, **Shimmen, T.**, & **Okada, K.** (2003). An Arabidopsis ACT2 dominant-negative mutation, which disturbs F-actin polymerization, reveals its distinctive function in root development. *Plant and Cell Physiology*, **44**, 1131–1140.

Palevitz, B. A. (1987). Actin in the preprophase band of Allium cepa. *The Journal of Cell Biology*, **104**, 1515–1519. 104.6.1515 104.6.1515

Sano, T., **Higaki, T.**, **Oda, Y.**, **Hayashi, T.**, & **Hasezawa, S.** (2005). Appearance of actin microfilament 'twin peaks' in mitosis and their function in cell plate formation, as visualized in tobacco BY-2 cells expressing GFP-fimbrin. *The Plant Journal*, **44**, 595–605. https://doi.org/10.1111/j.1365-313X.2005.02558.x

Schaefer, E., **Belcram, K.**, **Uyttewaal, M.**, **Duroc, Y.**, **Goussot, M.**, **Legland, D.**, **Laruelle, E.**, **de Tauzia-Moreau, M. L.**, **Pastuglia, M.**, & **Bouchez, D.** (2017). The preprophase band of microtubules controls the robustness of division orientation in plants. *Science*, **356**, 186–189. https://doi.org/10.1126/science.aal3016

Schwab, B., **Mathur, J.**, **Saedler, R.**, **Schwarz, H.**, **Frey, B.**, **Scheidegger, C.**, & **Hülskamp, M.** (2003). Regulation of cell expansion by the DISTORTED genes in *Arabidopsis thaliana*: Actin controls the spatial organization of microtubules. *Molecular Genetics and Genomics*, **269**, 350–360.

Simon, M. L., **Platre, M. P.**, **Marques-Bueno, M. M.**, **Armengot, L.**, **Stanislas, T.**, **Bayle, V.**, **Caillaud, M. C.**, & **Jaillais, Y.** (2016). A PtdIns(4)P-driven electrostatic field controls cell membrane identity and signalling in plants. *Nature Plants*, **2**, 16089. https://doi.org/10.1038/nplants.2016.89

Smertenko, A. P., **Deeks, M. J.**, & **Hussey, P. J.** (2010). Strategies of actin reorganisation in plant cells. *Journal of Cell Science*, **123**, 3019–3028. http://dx.doi.org/10.1242/jcs.071126

Smith, L. G. (1999). Divide and conquer: Cytokinesis in plant cells. *Current Opinion in Plant Biology*, **2**, 447–453.

Staehelin, L. A., & **Hepler, P. K.** (1996). Cytokinesis in higher plants. *Cell*, **84**, 821–824.

Staiger, C. J., **Goodbody, K. C.**, **Hussey, P. J.**, **Valenta, R.**, **Drobak, B. K.**, & **Lloyd, C. W.** (1993). The profilin multigene family of maize: Differential expression of three isoforms. *The Plant Journal: For Cell and Molecular Biology*, **4**, 631–641.

Stockle, D., **Herrmann, A.**, **Lipka, E.**, **Lauster, T.**, **Gavidia, R.**, **Zimmermann, S.**, & **Muller, S.** (2016). Putative RopGAPs impact division plane selection and interact with kinesin-12 POK1. *Nature Plants*, **2**, 16120. https://doi.org/10.1038/nplants.2016.120

Takeuchi, M., **Karahara, I.**, **Kajimura, N.**, **Takaoka, A.**, **Murata, K.**, **Misaki, K.**, **Yonemura, S.**, **Staehelin, L. A.**, & **Mineyuki, Y.** (2016). Single microfilaments mediate the early steps of microtubule bundling during preprophase band formation in onion cotyledon epidermal cells. *Molecular Biology of the Cell*, **27**, 1809–1820. https://doi.org/10.1091/mbc.E15-12-0820

Team, R. C. (2019). R version 3.5. 3: A language and environment for statistical computing. R Foundation for Statistical Computing, Austria, Vienna.

Tejos, R., **Sauer, M.**, **Vanneste, S.**, **Palacios-Gomez, M.**, **Li, H.**, **Heilmann, M.**, **van Wijk, R.**, **Vermeer, J. E.**, **Heilmann, I.**, **Munnik, T.**, & **Friml, J.** (2014). Bipolar plasma membrane distribution of Phosphoinositides and their requirement for auxin-mediated cell polarity and patterning in Arabidopsis. *The Plant Cell*, **26**, 2114–2128. https://doi.org/10.1105/tpc.114.126185

Voigt, B., **Timmers, A. C.**, **Samaj, J.**, **Muller, J.**, **Baluska, F.**, & **Menzel, D.** (2005). GFP-FABD2 fusion construct allows in vivo visualization of the dynamic actin cytoskeleton in all cells of Arabidopsis seedlings. *European Journal of Cell Biology*, **84**, 595–608. https://doi.org/10.1016/j.ejcb.2004.11.011

Walker, K. L., **Muller, S.**, **Moss, D.**, **Ehrhardt, D. W.**, & **Smith, L. G.** (2007). Arabidopsis TANGLED identifies the division plane throughout mitosis and cytokinesis. *Current Biology*, **17**, 1827–1836. https://doi.org/10.1016/j.cub.2007.09.063

Wickham, H., **Chang, W.**, & **Wickham, M. H.** (2016). Package 'ggplot2'. *Create elegant data visualisations using the grammar of graphics*. Version, **2**(1), 1–189.

Wu, S. Z., & **Bezanilla, M.** (2014). Myosin VIII associates with microtubule ends and together with actin plays a role in guiding plant cell division. *eLife*, **3**, e03498. https://doi.org/10.7554/eLife.03498

Xu, X. M., **Zhao, Q.**, **Rodrigo-Peiris, T.**, **Brkljacic, J.**, **He, C. S.**, **Muller, S.**, & **Meier, I.** (2008). RanGAP1 is a continuous marker of the Arabidopsis cell division plane. *Proceedings of the National Academy of Sciences of the United States of America*, **105**, 18637–18642. https://doi.org/10.1073/pnas.0806157105

Yoneda, A., **Akatsuka, M.**, **Kumagai, F.**, & **Hasezawa, S.** (2004). Disruption of actin microfilaments causes cortical microtubule disorganization and extraphragmoplast formation at M/G1 interface in synchronized tobacco cells. *Plant & Cell Physiology*, **45**, 761–769. https://doi.org/10.1093/pcp/pch091